ADVANCES IN NUCLEAR SCIENCE AND APPLICATIONS

Volume 1, No. 3 (2025) 151-161

The covariant confined quark model as a unified tool for heavy hadron decays

Z. Tyulemissov[*,1,2], A. Tyulemissova[2]

[1]Institute of Nuclear Physics, Almaty, Kazakhstan

[2]Joint Institute for Nuclear Research, Dubna, Russia

e-mail: zhomart@theor.jinr.ru

DOI: 10.63907/ansa.v1i3.55
Received: 20 September 2025

Abstract

We present a comprehensive study of the Covariant Confined Quark Model (CCQM), a versatile framework for describing electromagnetic, semileptonic, and nonleptonic decays of heavy mesons and quarkonia. The CCQM is built on a covariant nonlocal quark–hadron interaction Lagrangian that incorporates confinement through vertex functions while preserving gauge invariance. We outline the construction of matrix elements for a wide range of decay processes and emphasize the model's ability to reproduce decay widths in good agreement with experimental data. The parameters of the model are fixed using known meson masses and decay constants, thereby demonstrating the predictive power of the CCQM in heavy-flavor physics.

Introduction

The study of heavy mesons and quarkonia decays plays a crucial role in understanding the dynamics of strong and weak interactions within the Standard Model of particle physics. These processes provide sensitive tests of Quantum Chromodynamics (QCD), especially in its nonperturbative regime where quark confinement and hadronization phenomena dominate. Despite significant progress, the theoretical description of such decays remains challenging due to the complexity of nonperturbative effects. Various theoretical approaches, including lattice QCD simulations [1, 2], QCD sum rules [3],

and effective field theories [4,5], have been developed to tackle these challenges, each with its advantages and limitations.

One ongoing debate concerns the optimal way to incorporate quark confinement and hadron structure into phenomenological models. While local quark models often lack gauge invariance and struggle with ultraviolet divergences, nonlocal approaches have shown promise in addressing these issues. The Covariant Confined Quark Model (CCQM) [6–8] offers a fully covariant, gauge-invariant framework that introduces nonlocal vertex functions to simulate quark confinement effectively. Although the CCQM is widely used to describe the decays of heavy mesons and quarkonia, it has also been successfully applied to processes in the light hadron sector, including hadrons composed of u, d, s, and c quarks. For instance, in [9], two-body nonleptonic decays of light Λ-hyperon, $\Lambda \to p\pi^-(n\pi^0)$, were systematically studied, accounting for both short- and long-distance effects. The short-distance effects are induced by five topologies of external and internal weak $W^\pm$-exchange, while long-distance effects are saturated by an inclusion of the so-called pole diagrams with intermediate $\frac{1}{2}^+$- and $\frac{1}{2}^-$-baryon resonances. The contributions from $\frac{1}{2}^+$ resonances were calculated straightforwardly by account for nucleon and Σ-baryons, whereas the contributions from $\frac{1}{2}^-$ resonances were calculated by using the well-known soft-pion theorem in the current-algebra approach. This allows one to express the parity-violating $S-$ wave amplitude in terms of parity-conserving matrix elements. It was found that the contribution of external and internal W-exchange diagrams is sizably suppressed, e.g., by one order of magnitude in comparison with data, which are known with quite good accuracy. Pole diagrams play the major role in achieving consistency with experiment. Moreover, the model was applied to the strong decays of Δ-isobar, composed of $u-$ and $d-$-quarks [10]. In that paper we used the same mechanism for fitting the free parameter of the model to determine the decay width. The resulting behavior of the strong form factor $G_{\Delta p\pi}(Q^2)$ for space-like squared transferred pion momentum agrees well with other theoretical approaches and lattice calculations. Earlier works, such as Refs. [6,11], further demonstrate the applicability of the CCQM to both the light and heavy hadron sectors. This applicability is summarized in Table IV of Ref. [6], which lists various electromagnetic and leptonic decays.

In this work, we employ the CCQM to study electromagnetic, semileptonic, and nonleptonic decays of heavy mesons and quarkonia. Our main aim is to test the predictive power of the CCQM by calculating decay widths and form factors and comparing them with available experimental data. This approach allows us to assess the model's capacity to describe a wide range of heavy-flavor processes within a unified framework.

The paper is structured as follows: Section 1 presents the theoretical foundations of the CCQM, including the compositeness condition and the treatment of gauge invariance. Section 2 discusses the calculation of decay amplitudes. Section 3 describes the parameter fitting procedures. Finally, Section 4 summarizes our main conclusions and outlines prospects for future research.

1 The Covariant Confined Quark Model (CCQM)

In this paper we consider the Covariant Confined Quark Model (CCQM) as a unified tool for electromagnetic, semileptonic and nonleptonic decays of the heavy mesons

and quarkonia.

The cornerstone of the CCQM mathematical apparatus is an invariant quark-hadron nonlocal interaction Lagrangian:

$$\mathcal{L}_{\rm int} = g_M M(x) J_M(x) + \text{H.c.}, \tag{1}$$

$$J_M(x) = \int dx_1 \int dx_2 \, F_M(x; x_1, x_2) \bar{q}_2(x_2) \Gamma_M q_1(x_1), \tag{2}$$

where g_M is the coupling constant of the hadron field M and the quark current J_M, F_M is a vertex function and Γ_M the appropriate string of Dirac matrices which corresponds to the spin and parity of the meson. The vertex function is taken as an exponential term (to incorporate the hadron size) multiplied by a delta function (to ensure translational invariance)

$$\begin{aligned} F_M(x; x_1, x_2) &= \delta(x - \omega_1 x_1 - \omega_2 x_2) \Phi_M \left[(x_1 - x_2)^2 \right], \\ \omega_{1,2} &= m_{1,2} / \left(m_1 + m_2 \right), \\ \Phi_M \left[(x_1 - x_2)^2 \right] &= \int \frac{d^4k}{(2\pi)^4} e^{-ik(x_1 - x_2)} \tilde{\Phi}(-k^2), \\ \tilde{\Phi}(-k^2) &= e^{k^2/\Lambda_M^2}. \end{aligned}$$

Here, Λ_M is a size parameter of the model, which is fixed by the well-known meson mode. m_i are quark masses and $\tilde{\Phi}$ represents the Fourier-transformed vertex function. The exponential form of the vertex function helps to avoid any of ultraviolet divergences. To guarantee convergence in the CCQM, a cutoff via the Schwinger parameter is introduced Ref. [6, 7]. It should be noted that in the case when the meson mass is heavier than the sum of constituent quark masses, there are no infrared divergences, and integrals can be calculated without this mechanism.

The coupling constant can be determined from the compositeness condition, which is formulated in terms of the derivative of the meson mass operator. This condition serves as the main mechanism for eliminating double counting of quark degrees of freedom

$$Z_M = 1 - g_M^2 \Pi_M^{'}(m_M^2) = 0. \tag{3}$$

The renormalization constant Z_M is interpreted as a measure of the mixing between a physical meson state and its corresponding bare state. Setting $Z_M = 0$ effectively excludes any bare state component from the physical state, allowing the meson to be understood as a fully bound quark-antiquark system (see Refs. [6, 8]). Within this framework, quarks appear only as internal constituents mediating interactions: the meson may momentarily dissociate into a virtual quark pair during the interaction process and subsequently recombine into a meson in the final state. The coupling constant g_M is then adjusted to satisfy the condition expressed in Eq. (3). Notably, gluonic degrees of freedom are not included explicitly in the model; instead, their effects are absorbed into the structure of the vertex function, which depends on model parameters. The mass functions can be written explicitly as

$$\widetilde{\Pi}_P(p^2) = N_c g_P^2 \int \frac{d^4k}{(2\pi)^4 i} \widetilde{\Phi}_P^2(-k^2) \text{Tr}\Big(\gamma^5 S_1(k + w_1 p) \gamma^5 S_2(k - w_2 p) \Big), \tag{4}$$

$$\begin{aligned} \widetilde{\Pi}_V^{\mu\nu}(p^2) &= N_c g_V^2 \int \frac{d^4k}{(2\pi)^4 i} \widetilde{\Phi}_V^2(-k^2) \text{Tr}\Big(\gamma^\mu S_1(k + w_1 p) \gamma^\nu S_2(k - w_2 p) \Big) \\ &= g^{\mu\nu} \widetilde{\Pi}_V(p^2) + p^\mu p^\nu \widetilde{\Pi}_V^{\parallel}(p^2). \end{aligned} \tag{5}$$

Here $N_c = 3$ is the number of colors. Since the vector meson is on its mass-shell $\epsilon_V \cdot p = 0$ we need to keep the part $\widetilde{\Pi}_V(p^2)$. Substituting the derivative of the mass functions into Eq. (3) one can determine the coupling constant g_B as a function of other model parameters.

The electromagnetic interaction can be incorporated into the CCQM in a way that respects gauge symmetry. To achieve this, one introduces a gauge-field exponential $I(x_i, x, P)$, which is defined as a path-independent integral

$$q(x_i) \to Q(x_i) = e^{-ie_q I(x_i,x,P)} q(x_i) \tag{6}$$

$$\bar{q}(x_i) \to \bar{Q}(x_i) = \bar{q}(x_i) e^{ie_q I(x_i,x,P)} \tag{7}$$

$$I(x_i, x, P) = \int_x^{x_i} dz_\mu A^\mu(z) \tag{8}$$

where P is a path between x_i and x. In what follows, we focus on the first derivatives of $I(x_i, x, P)$, see [6, 12]. Using the definition of the derivative, one obtains:

$$\frac{\partial}{\partial x^\mu} I(x, y, P) = A_\mu(x).$$

2 Matrix elements

The main focus of this paper is the study of various decay processes of heavy mesons and quarkonia. These decays fall into three distinct categories: electromagnetic, nonleptonic, and semileptonic. Accordingly, three types of matrix elements are considered. Each class of decay processes is described by a corresponding matrix element that encodes the dynamics of the underlying quark-level transitions and their hadronization into observable meson states. These matrix elements are constructed within the framework of quantum field theory using time-ordered products of interpolating currents. The general structure involves meson-quark couplings, polarization vectors of external mesons or photons, and relevant interaction operators, such as the electromagnetic current or the effective weak Hamiltonian. Below, we present the explicit forms of the matrix elements for representative decay processes in each category:

$$\begin{aligned} M_{VP\gamma}(p; p', q) = {} & e g_V g_P \, \epsilon_\nu^V(p) \epsilon_\mu^\gamma(q) \int dx \int dy \int dz \, e^{-ipx+ip'y+iqz} \\ & \times \left\langle T\{\bar{J}_V^\nu(x) J_{\rm em}^\mu(z) J_P(y)\} \right\rangle_0, \end{aligned} \tag{9}$$

$$\begin{aligned} M_{V\gamma}(p, q) = {} & e g_V \epsilon_\nu^V(p) \epsilon_\mu^\gamma(q) \int dx \int dz \, e^{-ipx+iqz} \\ & \times \left\langle T\{\bar{J}_V^\nu(x) J_{\rm em}^\mu(z)\} \right\rangle_0, \end{aligned} \tag{10}$$

$$\begin{aligned} M_{VV_1V_2}(p; p', q) = {} & g_V g_{V_1} g_{V_2} \, \epsilon_\alpha^V(p) \epsilon_\beta^{V_1}(p_1) \epsilon_\gamma^{V_2}(q) \\ & \times \int dx \int dy \int dz \, e^{-ipx+ip'y+iqz} \\ & \times \left\langle T\{\bar{J}_V^\alpha(x) H_{eff} J_{V_1}^\beta(y) J_{V_2}^\gamma(z)\} \right\rangle_0. \end{aligned} \tag{11}$$

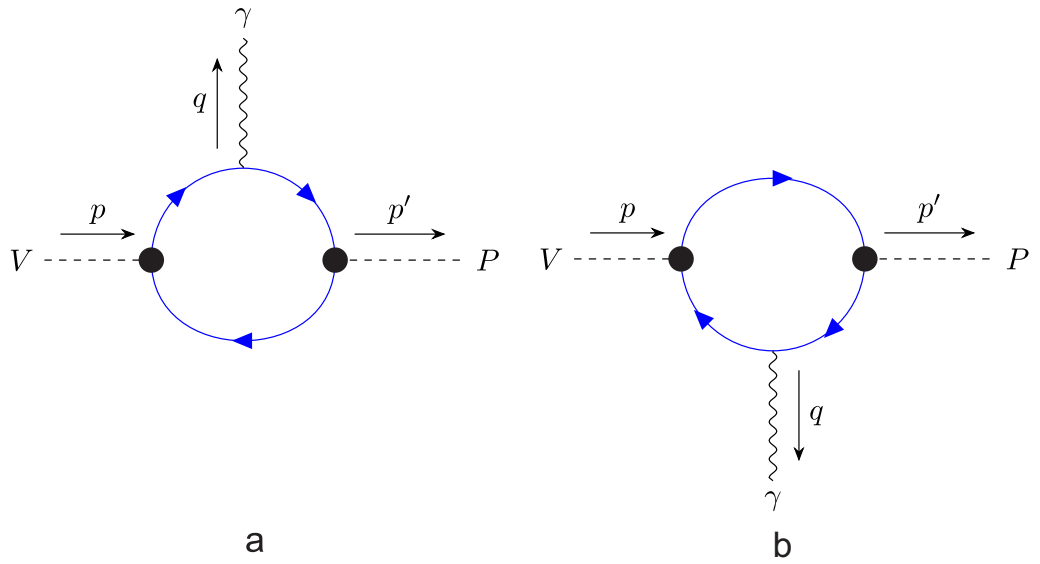

Figure 1: Feynman diagrams describing the radiative decays of a vector meson.

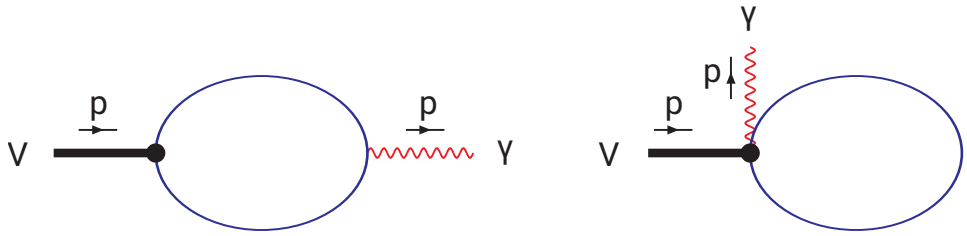

Figure 2: Feynman diagrams describing the $V \to \gamma$ decay of a vector meson.

Here:

$$J^{\mu}_{\rm em}(z) = \int d\rho\, \Phi_M(\rho^2)\, iee_q\, [I_z^{z_2} - I_z^{z_1}],$$

$$H_{eff} = -\frac{G_F}{\sqrt{2}} V^*_{cb} V_{q_1 q_2} \Big(C_2\, (\bar{c}_a O^{\mu} b_a)(\bar{q}_{1b} O_{\mu} q_{2b}) + C_1\, (\bar{c}_a O^{\mu} b_b)(\bar{q}_{1b} O_{\mu} q_{2a}) \Big).$$

All relevant Feynman diagrams are shown in Fig. 1-3. The matrix elements above are expressed in coordinate space. To compute their numerical values, one must apply a Fourier transformation and transition to momentum space. Consequently, in the momentum space these matrix elements take the following form:

- matrix element of the electromagnetic decay

$$M_{VP\gamma}(p;p',q) = (2\pi)^4 i\, \delta(p-p'-q) M(p,p'), \tag{12}$$

$$M(p,p') = (-3i) e g_V g_P \epsilon^V_{\nu}(p) \epsilon^{\gamma}_{\mu}(q) \left(e_b M^{\mu\nu}_b + e_q M^{\mu\nu}_q \right)$$

$$M^{\mu\nu}_b = \int \frac{dk}{(2\pi)^4 i} \widetilde{\Phi}_V(-\ell_1^2) \widetilde{\Phi}_P(-\ell_2^2) {\rm Tr} \left[S_q(k) \gamma^{\nu} S_b(k-p) \gamma^{\mu} S_b(k-p') \gamma^5 \right]$$

$$M^{\mu\nu}_q = \int \frac{dk}{(2\pi)^4 i} \widetilde{\Phi}_V(-\ell_3^2) \widetilde{\Phi}_P(-\ell_4^2) {\rm Tr} \left[S_q(k+p') \gamma^{\mu} S_q(k+p) \gamma^{\nu} S_b(k) \gamma^5 \right]$$

Here, $\ell_1 = k - w_2\, p$, $\ell_2 = k - w_2\, p'$ and $\ell_3 = k + w_1\, p$, $\ell_2 = k + w_1\, p'$. In the case of a massless photon, Maxwell's equations together with gauge invariance

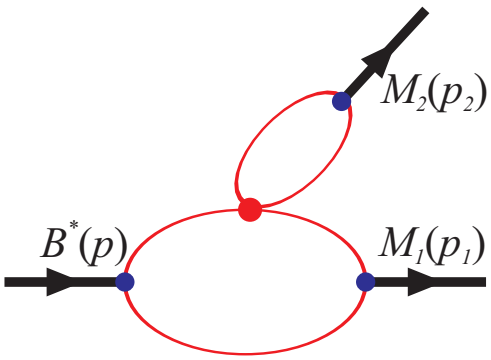

Figure 3: Feynman diagrams describing the nonleptonic decay of a vector meson.

lead to the transversality condition $\epsilon^{\gamma}_{\mu}(q)q^{\mu} = 0$. In vector meson decays, the transversality condition $\epsilon^{V}_{\nu}(p)p^{\nu} = 0$ must also be imposed in order to exclude longitudinal components from the physical polarization. Accordingly, the matrix element that incorporates this condition takes the following form

$$M(p,p') = e\, g_{VP\gamma}\, \varepsilon^{pq\mu\nu} \epsilon^{\gamma}_{\mu}(q) \epsilon^{V}_{\nu}(p),$$

where $g_{VP\gamma} = e_b I_b(m_V^2, m_P^2) + e_q I_q(m_V^2, m_P^2)$ is radiative decay constant. The quantities $I_{b,q}$ are defined by the double-fold integrals which are calculated numerically.

- matrix element of the electromagnetic decay $V(p) \to \gamma(p)$

$$M^{\mu\nu}(V(p) \to \gamma(p)) = N_c g_V \int \frac{d^4k}{(2\pi)^4 i} \Big\{ \Phi_V(-k^2)\, \mathrm{tr}\Big[\gamma^{\mu} S(k + \tfrac{1}{2}p)\, \gamma^{\nu} S(k - \tfrac{1}{2}p)\Big] - \int_0^1 d\tau\, \Phi'_V(-z_\tau)(2k + \tfrac{1}{2}p)^{\mu} \mathrm{tr}\Big[\gamma^{\nu} S(k)\Big] \Big\}, \tag{13}$$

$$z_\tau = \tau\Big(k + \tfrac{1}{2}p\Big)^2 + (1-\tau)k^2. \tag{14}$$

Here, N_c is the number of colors, and g_V is the coupling constant associated with the vector meson. The function Φ_V represents the vertex form factor describing the internal structure of the meson, with Φ'_V denoting its derivative with respect to the argument. The integral over the Feynman parameter τ appears due to the nonlocal nature of the vertex function and ensures gauge invariance of the matrix element by properly accounting for the momentum dependence of the vertex.

- matrix element of the nonleptonic decay

$$\begin{aligned} M(B^*(p) \to M_1(p_1) M_2(p_2)) = {} & \frac{G_F}{\sqrt{2}} V_{CKM} a_W\, m_2 f_{M_2}\, \epsilon_{2\,\mu} \\ & \times N_c\, g_{B^*}\, g_{M_1}\, \epsilon_{\alpha}(p)\, \epsilon^{*}_{1\,\beta}(p_1) \\ & \times \int \frac{d^4k}{(2\pi)^4 i}\, \widetilde{\Phi}_{B^*}\Big(- (k + w_{13} p_1)^2 \Big) \\ & \times \widetilde{\Phi}_{M_1}\Big(- (k + w_{23} p_2)^2 \Big) \\ & \times \mathrm{Tr}\Big[O^{\mu}\, S_1(k + p_1)\, \gamma^{\alpha}\, S_3(k)\, \gamma^{\beta}\, S_2(k + p_2) \Big]. \end{aligned} \tag{15}$$

The nonleptonic decay is mediated by the effective weak interaction, characterized by the Fermi coupling constant G_F, the relevant Cabibbo-Kobayashi-Maskawa (CKM) matrix elements V_{CKM}, and the factor a_W, which accounts for short-distance QCD effects. The term $m_2 f_{M_2} \epsilon_{2\,\mu}$ corresponds to the leptonic decay constant and polarization vector of the meson M_2, together with its mass. The quark propagators S_i appear inside the trace along with the weak interaction operator O^μ, encoding the spinor structure of the process. The parameters $w_{ij} = m_{q_j}/(m_{q_i} + m_{q_j})$ are introduced to reflect the relative contributions of constituent quark masses within the mesons, allowing for a proper treatment of the internal dynamics in the loop integral.

Finally, based on matrix elements we obtain decay width of following processes:

$$\Gamma(V \to P + \gamma) = \frac{\alpha}{24} m_V^3 \left(1 - \frac{m_P^2}{m_V^2}\right)^3 g_{VP\gamma}^2 \,. \tag{16}$$

$$\Gamma(V \to \ell^+ \ell^-) = \frac{4\pi\alpha^2}{3}\, m_V \Big(\frac{Q_V f_V}{m_V}\Big)^2 \sqrt{1 - 4x_\ell^2}\,(1 + 2x_\ell^2), \tag{17}$$

$$\Gamma\left(B^{*\,\lambda} \to M_1^{\lambda_1} M_2^{\lambda_2}\right) = \frac{|\mathbf{p_2}|}{24\pi\, M^2} \sum_{\lambda_1 \lambda_2} |M(B^* \to M_1 M_2)|^2 \tag{18}$$

where $\lambda = -\lambda_1 + \lambda_2$ is the helicity configuration of the decay products, and $|\mathbf{p}_2|$ is the magnitude of the final-state meson momentum in the rest frame of the decaying particle. In the expression for the electromagnetic decay $V \to P + \gamma$, the form factor $g_{VP\gamma}$ characterizes the coupling constant between the vector and pseudoscalar mesons and the photon. In the leptonic decay width $\Gamma(V \to \ell^+\ell^-)$, the factor $f_V \equiv G_V(m_V^2)/m_V$ represents the leptonic decay constant of the vector meson, which in our convention coincides with the weak decay constant. The variable $x_\ell = m_\ell/m_V$ denotes the lepton mass normalized to the meson mass. The quark charge factor Q_V depends on the flavor composition of the meson: $Q_V = (e_u - e_d)/\sqrt{2} = 1/\sqrt{2}$ for the ρ^0 meson, $Q_V = e_c = 2/3$ for charmonium (J/ψ), and $Q_V = e_b = -1/3$ for bottomonium (Υ) states. These formulas provide the final step in connecting theoretical amplitudes with observable quantities and serve as the basis for comparison with experimental data.

3 The model parameters

We begin by listing the fixed parameters of the CCQM, as taken from the Particle Data Group (PDG) [13]. Table 1 shows the constituent quark masses used in the model, along with the universal infrared cutoff parameter λ, which was determined in earlier works (see Ref. [8] for details).

Table 1: Model parameters: quark masses and cutoff parameter λ (all in GeV).

m_u	m_s	m_c	m_b	λ
0.241	0.428	1.67	5.04	0.181

The masses of the ground and radially excited states of the mesons and quarkonium are given in Table 2.

Table 2: Masses of heavy meson taken from the PDG [13] (in MeV).

$B^{\pm}$	B^0	B_s^0	B_c^+	B^*
5279.25(26)	5279.63(20)	5366.91(11)	6274.47(32)	5324.71(21)

B_s^*	J/Ψ	$\Upsilon(1s)$
5415.8(1.5)	3096.900(6)	9460.30(26)

Only 10 free parameters are used to describe the 21 exclusive decay channels considered in this paper. Table 3 presents the fitted size parameters for the vector mesons involved in this work. The fitting of these parameters was performed primarily

Table 3: Size parameters of vector mesons and quarkonia (in GeV)

Λ_ρ	Λ_{K^*}	Λ_{D^*}	$\Lambda_{D_s^*}$	Λ_{B^*}	$\Lambda_{B_s^*}$	$\Lambda_{J/\Psi}$	Λ_Υ
0.61	0.81	1.53	1.56	1.72	1.71	2.795	4.03

based on the leptonic decay constants of the mesons. The size parameters Λ_M were adjusted such that the decay constants calculated within the CCQM framework agree with available experimental measurements. In cases where experimental data were lacking, lattice QCD results were used as benchmarks to guide the fitting procedure. This ensures that the model consistently reproduces key observables across different meson families. All numerical values for the leptonic decay constants used in the fit are listed in Table 4. The numerical values obtained within the CCQM for the

Table 4: Calculated leptonic decay constants f_{M_2} (in MeV).

	CCQM	Expt/Lat	
f_ρ	218(22)	221(1)	[13]
f_{K^*}	227(23)	217(7)	[13]
f_{D^*}	246(25)	223.5(8.4)	[1]
$f_{D_s^*}$	273(27)	268.8(6.6)	[1]
f_{B^*}	185(19)	186.4(7.1)	[1,2]
$f_{B_s^*}$	260(26)	223.1(5.6)	[1,2]
$f_{J/\psi}$	415(42)	405(6)	[14]
$f_{\Upsilon(1S)}$	700(70)	689.7(4.6)	[15]

leptonic decay constants are in excellent agreement with both experimental and lattice QCD data. The next step is to numerically compute the decay widths for electromagnetic, leptonic, and nonleptonic processes of the heavy vector mesons and quarkonia.

4 Results and discussion

First, in Table 5 and 6 we present widths of electromagnetic decay obtained by CCQM based on the previously fixed parameters. Our results are compared with

those from various other theoretical approaches available in the literature. As seen

Table 5: Widths of $B^* \to B\gamma$ and $B_s^* \to B_s\gamma$ decays (in eV).

Mode	CCQM	[16]	[17]	[18]	[19]	[3]
$B^{*+} \to B^+\gamma$	372(56)	349(18)	400(30)	190	740(88)	380(60)
$B^{*0} \to B^0\gamma$	126(19)	116(6)	130(10)	70	228(27)	130(30)
$B_s^{*0} \to B_s^0\gamma$	90(14)	84(10)	68(17)	54	136(12)	220(40)

Mode	CCQM	[20]	[4]
$B^{*+} \to B^+\gamma$	372(56)	401	220(90)
$B^{*0} \to B^0\gamma$	126(19)	131	75(27)

Table 6: Widths of $B_c^* \to B_c\gamma$ decay (in eV).

Mode	CCQM	[21]	[22]	[23]	[18]	[24]	[25]
$B_c^{*+} \to B_c^+\gamma$	33(5)	53(3)	80	59	33	60	135

from Tables 5 and 6, the CCQM predictions for radiative decay widths are generally consistent with those obtained in other theoretical models, although some spread in values exists due to differences in model assumptions and parameters. Our results provide a reliable estimate of electromagnetic decay widths for the B^*, B_s^*, and B_c^* mesons, which are important for understanding their structure and for comparison with future experimental data.

Table 7 presents the leptonic branching ratios of quarkonia. From the results

Table 7: Leptonic decay branching ratio of J/Ψ and $\Upsilon(1s)$-mesons

Quantity	J/ψ		$\Upsilon(1S)$	
$\mathcal{B}(V \to \ell^+\ell^-)$	CCQM	Expt	CCQM	Expt
$\mathcal{B}(V \to \tau^+\tau^-)$ (%)			2.365	2.60(10)
$\mathcal{B}(V \to \mu^+\mu^-)$ (%)	5.964	5.961(33)	2.384	2.38(5)
$\mathcal{B}(V \to e^+e^-)$ (%)	5.964	5.971(32)	2.384	2.48(11)

presented in Table 7, the model reproduces both the muon and electron decay channels with high precision. The decay to τ leptons is kinematically forbidden for J/ψ due to its mass but allowed and well described for the heavier $\Upsilon(1S)$ state. This agreement provides confidence in the CCQM approach for calculating leptonic decays of heavy quarkonia.

Conclusions

The Covariant Confined Quark Model (CCQM) provides a unified and consistent framework for studying the decays of heavy mesons and quarkonia. By combining

nonlocal quark–hadron interactions with the compositeness condition, it reproduces key observables such as decay widths and form factors in good agreement with experiment and lattice QCD. Certain processes, such as meson production in electron–positron annihilation ($e^+e^- \to M\bar{M}$), remain beyond its standard scope, since the model does not include the full dynamics of fragmentation or multi-hadron emission. Nevertheless, the gauge-invariant treatment of electromagnetic interactions and the careful fitting of parameters ensure that the CCQM captures essential aspects of hadron structure and dynamics. In addition to the methodological developments emphasized here, the approach has been successfully applied to electromagnetic [26], leptonic [27, 28], and nonleptonic [26, 29–31] B-meson decays. Overall, the CCQM confirms its value as a tool for heavy-flavor physics and offers prospects for further applications to more complex processes and hadronic states.

Acknowledgments

The authors would like to express their sincere gratitude to Stanislav Dubnička, Anna Zuzana Dubničková, Mikhail A. Ivanov, and Andrej Liptaj for their valuable assistance and fruitful discussions that greatly contributed to the development of this work. The research has been funded by the Science Committee of the Ministry of Science and Higher Education of the Republic of Kazakhstan (Grant No. AP19678771).

References

[1] V. Lubicz et al. [ETM], Phys. Rev. D **96**, no.3, 034524 (2017).

[2] A. Bussone et al. [ETM], Phys. Rev. D **93**, no.11, 114505 (2016).

[3] S.L. Zhu, W.Y.P. Hwang and Z.S. Yang, Mod. Phys. Lett. A **12**, 3027 (1997).

[4] P. Colangelo, F. De Fazio and G. Nardulli, Phys. Lett. B **316**, 555 (1993).

[5] J. Zeng, J.W. Van Orden and W. Roberts, Phys. Rev. D **52**, 5229 (1995).

[6] T. Branz, A. Faessler, T. Gutsche, M.A. Ivanov, J.G. Korner and V.E. Lyubovitskij, Phys. Rev. D **81**, 034010 (2010).

[7] G. Ganbold, T. Gutsche, M.A. Ivanov and V.E. Lyubovitskij, J. Phys. G **42**, no.7, 075002 (2015).

[8] S. Dubnička, A.Z. Dubničková, N. Habyl, M.A. Ivanov, A. Liptaj and G.S. Nurbakova, Few Body Syst. **57**, no.2, 121 (2016).

[9] M.A. Ivanov, J.G. Körner, V.E. Lyubovitskij and Z. Tyulemissov, Phys. Rev. D **104**, no.7, 074004 (2021).

[10] M.A. Ivanov, G. Nurbakova and Z. Tyulemissov, Phys. Part. Nucl. Lett. **15**, no.1, 1 (2018).

[11] A. Faessler, T. Gutsche, B.R. Holstein, M.A. Ivanov, J.G. Körner and V.E. Lyubovitskij, Phys. Rev. D **78**, 094005 (2008).

[12] T. Branz, A. Faessler, T. Gutsche, M.A. Ivanov, J.G. Körner, V.E. Lyubovitskij and B. Oexl, Phys. Rev. D **81**, 114036 (2010).

[13] R.L. Workman et al. [Particle Data Group], PTEP **2022**, 083C01 (2022).

[14] G.C. Donald, C.T.H. Davies, R.J. Dowdall, E. Follana, K. Hornbostel, J. Koponen, G.P. Lepage and C. McNeile, Phys. Rev. D **86**, 094501 (2012).

[15] D. Hatton, C.T.H. Davies, J. Koponen, G.P. Lepage and A.T. Lytle, Phys. Rev. D **103**, no.5, 054512 (2021).

[16] Q. Chang, Y. Zhang and X. Li, Chin. Phys. C **43**, no.10, 103104 (2019).

[17] H.M. Choi, Phys. Rev. D **75**, 073016 (2007).

[18] D. Ebert, R.N. Faustov and V.O. Galkin, Phys. Lett. B **537**, 241 (2002).

[19] J.L. Goity and W. Roberts, Phys. Rev. D **64**, 094007 (2001).

[20] M.A. Ivanov and Y.M. Valit, Z. Phys. C **67**, 633 (1995).

[21] C.W. Liu and B.D. Wan, Phys. Rev. D **105**, no.11, 114015 (2022).

[22] S. Godfrey, Phys. Rev. D **70**, 054017 (2004).

[23] L.P. Fulcher, Phys. Rev. D **60**, 074006 (1999).

[24] S.S. Gershtein, V.V. Kiselev, A.K. Likhoded and A.V. Tkabladze, Phys. Rev. D **51**, 3613 (1995).

[25] E.J. Eichten and C. Quigg, Phys. Rev. D **49**, 5845 (1994).

[26] M.A. Ivanov, Z. Tyulemissov and A. Tyulemissova, Phys. Rev. D **107**, no.1, 013009 (2023).

[27] S. Dubnička, A.Z. Dubničková, M.A. Ivanov and A. Liptaj, Symmetry **15**, no.8, 1542 (2023).

[28] C.T. Tran, M.A. Ivanov and A.T.T. Nguyen, Chin. Phys. C **49**, no.11, 113105 (2025).

[29] M.A. Ivanov, J.G. Körner, S.G. Kovalenko, P. Santorelli and G.G. Saidullaeva, Phys. Rev. D **85**, 034004 (2012).

[30] M.A. Ivanov, J.G. Körner and P. Santorelli, Phys. Rev. D **73**, 054024 (2006).

[31] M.A. Ivanov, J.G. Körner and O.N. Pakhomova, Phys. Lett. B **555**, 189 (2003).